Astron. Astrophys. 354, 909–914 (2000)

ASTRONOMY AND ASTROPHYSICS

Multicolour high-speed photometry and $H\alpha$ spectroscopy of XY UMa

D. Kjurkchieva[1], **D. Marchev**[1], **and W. Ogloza**[2,3]

[1] Department of Physics, Shoumen University, 9700 Shoumen, Bulgaria
[2] N.Copernicus Astronomical Center, Polish Academy of Sciences, ul.Bartycka 18, 00-716 Warszawa, Poland
[3] Mt. Suhora Observatory, Cracow Pedagogical University, ul.Podchorazych 2, 30-084 Cracow, Poland

Received 19 August 1998 / Accepted 20 July 1999

Abstract. BVRI photometry and $H\alpha$-line spectroscopy of the short-period RS CVn-binary XY UMa are presented. The light curves as a whole as well as the two eclipse minima are asymmetric. The light level after the primary minimum is lower by about 0.04-0.05 mag than that after the secondary one. Two cool spots on the primary with sizes 20° and 10°, temperatures 4630 and 4330 K at middle latitudes reproduced well the distortion curve in all colours. The observed $H\alpha$ profile is quite wide and asymmetric at most the phases out of the eclipses. The radial velocity curve is sinusoidal with semiamplitude $K_1 = 120.7 \pm 2.9$ km/s. The corresponding mass function of the system is $0.082 M_{\odot}$. The phase behaviour of the $H\alpha$-profile implies contribution of emission of the chromospheric regions above the photospheric spots.

Key words: publications, bibliography – book reviews – book reviews – stars: binaries: eclipsing – book reviews – stars: individual: XY UMa – book reviews – stars: luminosity function, mass function – book reviews – stars: starspots – Magnetohydrodynamics (MHD)

1. Introduction

The short-period RS CVn-stars (Hall 1976) form a particular subgroup of binary systems that exhibit observational signs of magnetic activity. The short periods means that these stars are relatively close to filling their Roche lobes. It is assumed (Rahunen & Vilhu 1982) that they will evolve ultimately into contact systems.

XY UMa (G3V+K3-5V) is a detached system but with the primary component filling a large fraction of its Roche volume (Rainger et al. 1991; Hilditch & Bell 1994). Budding & Zeilik (1987) estimate that the secondary component contributes about 5% of the system light. There is no trace of the secondary in the spectrum of XY UMa (Geyer 1976, Rainger et al. 1991).

The shape of the light curve of XY UMa is very variable. Geyer (1980) found that it alternates between the symmetrical and asymmetrical form within 3-4 years. But the BV photometry of Li et al. (1989) shows this change is only within a month.

Send offprint requests to: W. Ogloza (ogloza@astro.as.wsp.krakow.pl)

The variability of the light curve of XY UMa is exhibited by the following features: (a) brightness depression around some of the quadratures by 0.07 mag, more pointed at shorter wavelenghts; (b) asymmetry of the minima; (c) variable depth of the secondary eclipse that sometimes even disappears (Geyer 1977, Hilditch & Bell 1994) but sometimes reach a half depth of the primary (Zeilik et al. 1988); (d) definite trend for the whole system to become brighter (Hilditch & Collier Cameron 1995; Jeffries et al. 1995).

These photometric variations have been successfully interpreted by Geyer (1976, 1980) as being due to star spots over the surface of the primary component.

There are different signs of the high activity of XY UMa: flare activity (Zeilik et al. 1983); enhanced chromospheric emission (Geyer & Hoffman 1981); variable weak polarization (Geyer & Metz 1977); radio emission (Drake et al. 1986); soft X-ray emission (Singh et al. 1996); pecular IR light curve (Arevalo & Lazaro 1990).

In order to investigate the spot activity of XY UMa we carried out photometric and $H\alpha$ observations of the star.

2. Observations

2.1. Photometry

Our BVRI photometry of XY UMa was obtained at the end of 1996 by a two-channel photometer mounted on the 60-cm telescope (Kreiner et al. 1993) of the Mt.Suhora Observatory. In addition, V photometry of the star was carried out at the beginning of 1997 with the one-channel photometer of the 60-cm telescope of Belogradchik Observatory (Antov & Konstantinova-Antova 1995).

Table 1 gives the journal of our observations.

In order to satisfy the requirement of the two-channel photometer that the distance between the variable and comparison star should be in the range 10-20 arcmin, we have used the star $BD+55^{\circ}1321 = SAO27153$ (V=8.^{m}7) as a comparison star. A calibration of the channels and observation of the comparison star $SAO27105$ (V=5.^{m}6) were made every night. More details about the equipment and reduction procedure are given in Szymanski & Udalski (1989). The two-channel photometry was done using an autoguider (Krzesinski & Wojcik 1993). The

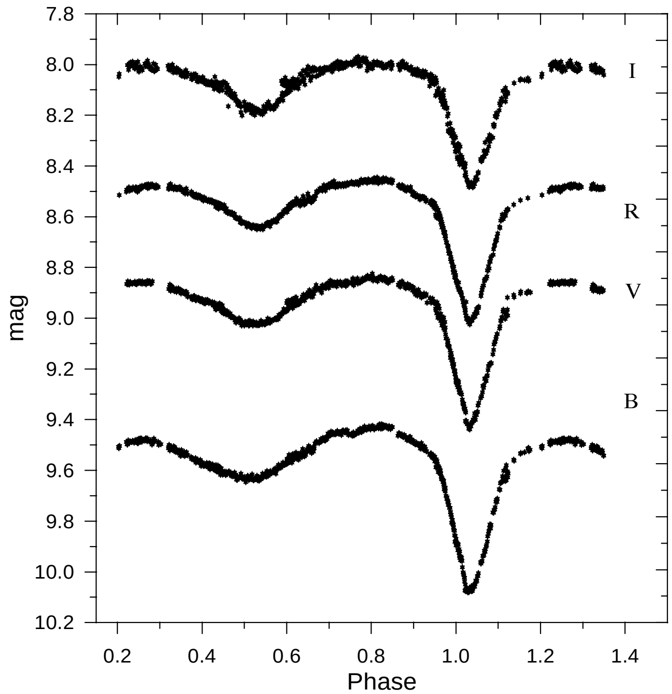

Fig. 1. Multicolour light curve of XY UMa at the end of 1996 (the data are phased according to the ephemeris (1)).

Table 1. Journal of observations

Date	HJD 2450000+	Spectral range	Phase range	Observatory
Nov 29 ’96	417	B,V,R,I	0.03-0.25	Mt.Suhora
Dec 3 ’96	421	B,V,R,I	0.60-1.00	Mt.Suhora
Dec 4 ’96	422	B,V,R,I	0.40-0.60	Mt.Suhora
Dec 5 ’96	422	B,V,R,I	0.90-1.10	Mt.Suhora
Dec 7 ’96	424	B,V,R,I	0.10-0.30	Mt.Suhora
Dec 11 ’96	429	B,V,R,I	0.27-0.42	Mt.Suhora
Feb 2 ’97	482	V	0.82-1.27	Belogradchik
Feb 3 ’97	483	V	0.70-1.35	Belogradchik
Feb 13 ’97	493	$H\alpha$	0.95-1.35	Rozhen
Feb 14 ’97	494	$H\alpha$	0.50-0.85	Rozhen
Feb 7 ’99	1216	$H\alpha$	0.4-0.66	Rozhen
Feb 9 ’99	1218	$H\alpha$	0.47-0.74	Rozhen

integration time was 10 sec in each filter. The same comparison stars were used during the one-channel observations. The internal error of the measurements did not exceed $0.^{m}01$ in all the colours.

The data were phased according to the ephemeris of Geyer et al. (1955):

$$HJD(MinI) = 2435216.5011 + 0.4789944 * E. \quad (1)$$

The light curves from our photometry are shown in Figs. 1-2.

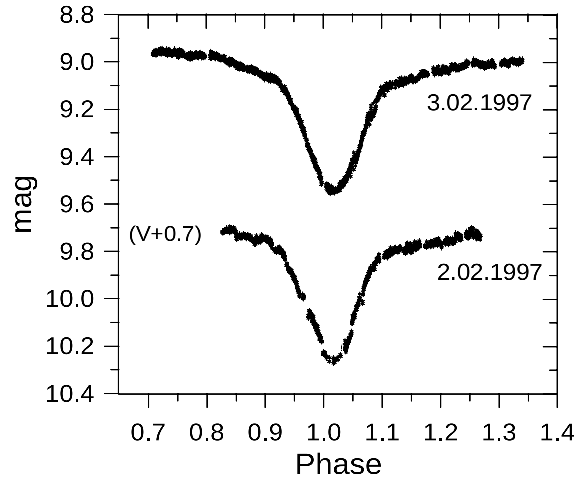

Fig. 2. V light curves of XY UMa at the beginning of 1997 (the data are phased according to the ephemeris (1)).

2.2. Spectroscopy

The $H\alpha$-line observations were obtained at the beginning of 1997 and at the beginning of 1999. We used a CCD camera mounted on the Coudé spectrograph (grating $B\&L632/14.7°$) of the 2-m telescope operated by the National Astronomical Observatory in Rozhen (Bulgaria). This provides an interval of $\Delta\lambda$=110 Å and a resolution of 0.19 Å/pix. The seeing during the observations did not exceed 2 arcsec (FWHM). The exposure time was 20 min. The bias frames and flat-field integrations were obtained at the beginning and end of each night. All stellar integrations were alternated with Fe comparison source exposures. The ratio S/N was around 25-30. The data were processed (bias, dark and flat frames) in a standard way using the PCIPS (Smirnov et al. 1992) and Rewia (Borkowski 1988) software packages. An appropriate Fourier noise filter was applied in order to remove the high-frequency noise. This procedure causes some smoothing of the profiles without loss of their main details (Gray 1992). The local continuum was normalized to 1 outside the line. The obtained $H\alpha$ profiles are shown in Figs. 3-4 together with the corresponding orbital phases.

3. Analysis of the photometric data

3.1. Times of minima and (O-C) diagram

The times of minima determined by fitting parabolas to the lower half of the eclipses of our curves are:

$$MinI = 2450422.6754 \pm 0.0001$$

$$MinII = 2450422.4364 \pm 0.0002 \quad (2)$$

$$MinI = 2450482.5526 \pm 0.0001$$

$$MinI = 2450483.5107 \pm 0.0001.$$

The first two values are determined from the multicolour photometry and the second two values are determined from Feb ’97

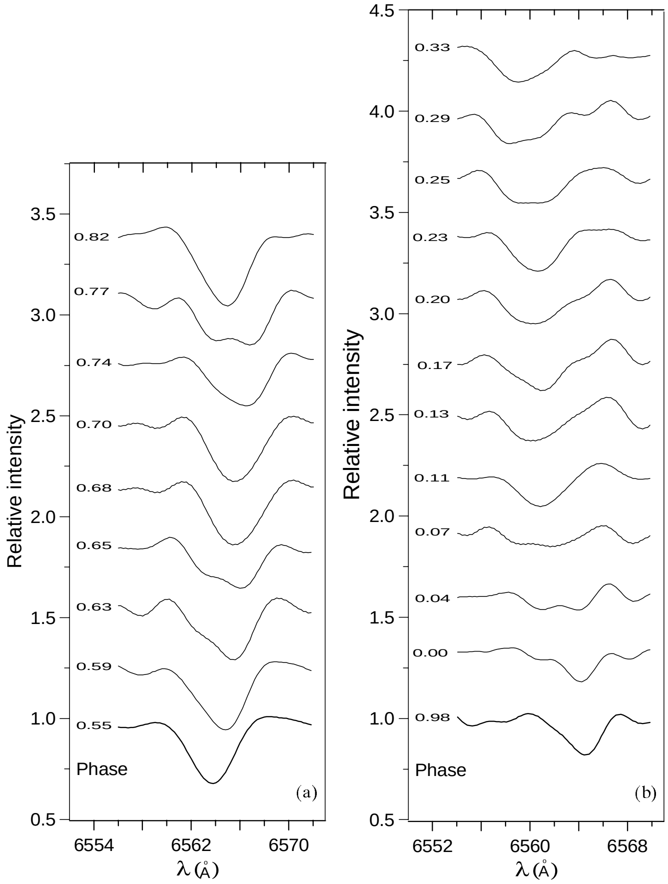

Fig. 3a and b. $H\alpha$ profile on February 13 **a** and 14 **b** 1997 (the phases are according to the ephemeris (1)).

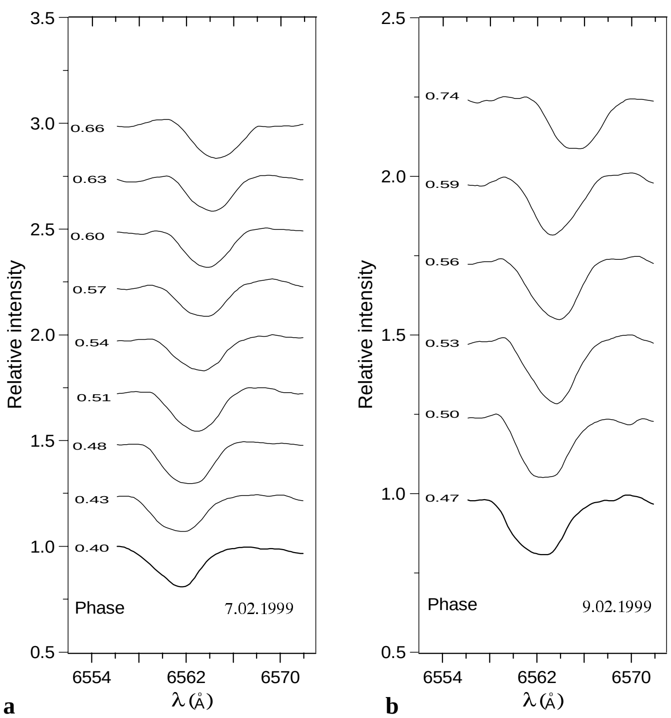

Fig. 4a and b. $H\alpha$ profile on February 7 (**a**) and 9 (**b**) 1999 (the phases are according to the ephemeris (1)).

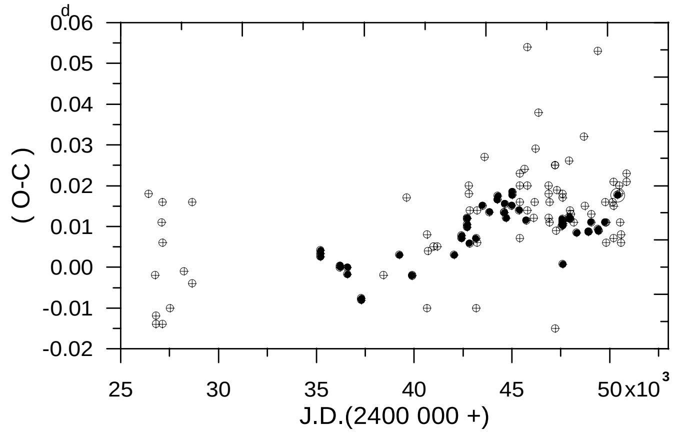

Fig. 5. (O-C) diagram according to the ephemeris (1). The sign • means photoelectric data; the sign ⊕ means photographic or visual data. Our point is marked additionally by circle (with the permission of Kreiner, priv.comm.).

V data. It should be noted that the times of the minima in the different colours coincide to within the errors.

The phase shift of our minima is 0.0374 with respect to the ephemeris (1). The (O-C) diagram built according to the ephemeris (1) on the base of the list of all minima compiled by Kreiner (private communication) is shown in Fig. 5.

There are different interpretations of the erratic changes and long-term changes of the orbital period of XY UMa (Hall & Kreiner 1980; Pojmanski & Geyer 1990; Erdem & Gudur 1998). Although the published O-C diagrams show a large scatter up to a value of $0^d.02$, the orbital period of XY UMa seems to be constant. We attribute this fact as well as the absence of any clear tendency in the behaviour of the (O-C) values (Fig. 5), to the nonuniform starspot distribution over the hemisphere that is eclipsed during the minima. Then the photometrically determined times of minima do not coincide with the ideal geometric ones.

3.2. Shape of the light curve

Our multicolour curve is characterized by the following features:

(1) The mean light level in the phase range 0.1-0.4 is lower by about 0.02-0.04 mag than that in the phase interval 0.6-0.9.

(2) The primary minimum is asymmetric. Its decreasing branch is much steeper than the increasing one. In the framework of the spot hypothesis this means the presence of a spot that is better visible after the bottom of the primary eclipse. The depths of the primary minima in the B, V, R and I bands are respectively 0.65, 0.59, 0.57, and 0.5 mag. They are slightly bigger than those observed by other authors (Zeilik et al. 1982; Zeilik et al. 1988; Li et al. 1989; Zeilik et al. 1990).

(3) The secondary minimum is quite distorted and asymmetric. The increasing branch of the eclipse is steeper than the decreasing one. The depths of the secondary minima in B, V, R and I colours are respectively 0.19, 0.195, 0.2, and 0.2 mag.

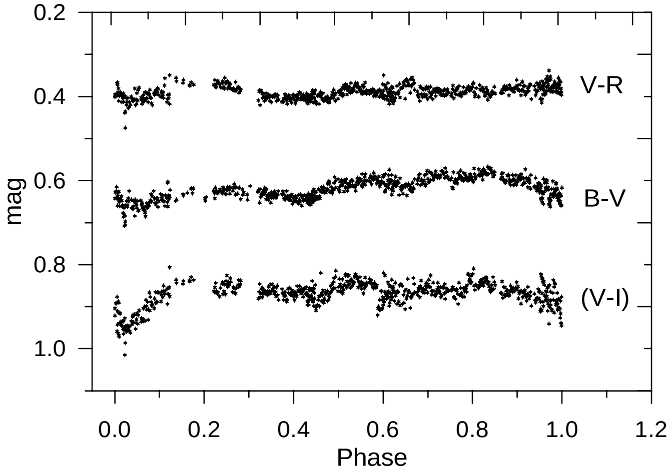

Fig. 6. Variations of colour indices with the orbital phase (according to the ephemeris (1)).

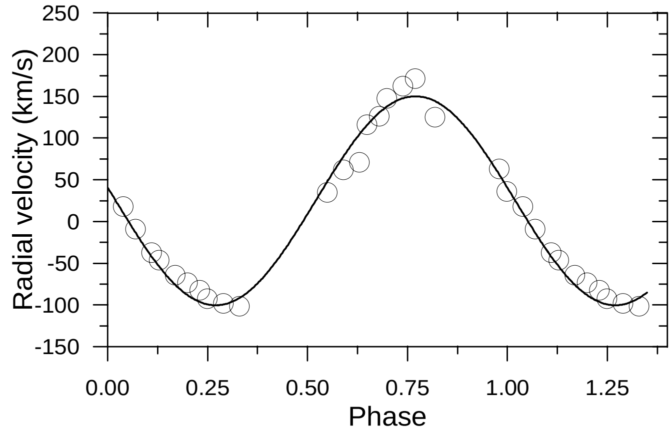

Fig. 7. Radial velocity curve of XY UMa on the base of $H\alpha$ line (the phases are according to the ephemeris (1)).

(4) The shapes of the light curves in the different colours are similar except for the bigger depression of the light in the B-band in the phase range 0.1-0.4 compared to the other colours.

The shape of our colour-difference curve (Fig. 6) means that the star becomes redder at the primary eclipse and bluer at the secondary eclipse than at the quadratures. This is in agreement with the spectral types of the two star components and means that the hotter component is also the larger one.

4. Analysis of the spectroscopic data

The observed $H\alpha$ profile of XY UMa is quite wide (7-8Å) and asymmetric at most phases outside the eclipses (Figs. 3-4). We noted the following faint tendency in the behaviour of the $H\alpha$ profile: during half the period (phase range 0.1-0.3) the left wing is steeper than the right one and during the other half the right wing is steeper than the left one.

Although its shape is variable, the $H\alpha$ line shows a relative stable width. This excludes the secondary component as a source of the observed orbital variability of the profile shape. The secondary star should cause doubling of the line out of the eclipses and stronger variations of its width.

Obviously, the primary star is the main source of the $H\alpha$ absorption. If its mass is $1M_{\odot}$ (appropriate to a G2-3V star) and the MS mass-radius relation is valid then the rotational velocity is around 100 km/s and the corresponding rotational broadening of its lines is around 4.4 Å. In fact, the observed $H\alpha$ profile is wider. We attribute this to the expansion of the primary star to its Roche lobe. For such cases the main-sequence mass-radius relation probably is not applicable (Southwell et al. 1995).

The radial velocity of the $H\alpha$ line was determined by fitting its profile with a 6th-order polynomial and measuring the position of the midpoint at half height. The error of the individual measurement does not exceed 5 km/s.

The spectral observations from 1999 cover a small part of the orbital cycle and cannot be used for a radial velocity curve. The radial velocity data from 1997 were fitted by least squares analysis using the VELFIT subroutine of the BINMAKER2 package (Bradstreet 1993) separately for 1997 and 1999. The sinusoidal fit (Fig. 7) provides a semi-amplitude for the primary component of $K_1 = 120.7 \pm 2.9$ km/s and a systematic velocity of $\gamma = 26 \pm 3.9$ km/s with a correlation coefficient 0.99.

Our K_1 value coincides to within the errors with Rainger's et al. (1991) value of 119.5 ± 2 km/s determined by measurement of the CaI 4226 line while our γ velocity value differs considerably from that of Rainger et al. (1991) ($\gamma = -9.2$ km/s). The reason is the lack of observations of standard stars in our spectral run.

The mass function of the system XY UMa corresponding to our K_1 value is $f(m)$=0.082 $M_{\odot}$.

More precise analysis of the orbital behaviour of the $H\alpha$ profile is impossible for the following reasons: (a) the low time resolution of the spectral observations; (b) the lack of phase coverage in the range 0.33-0.55 of our data; (c) the low ratio S/N of our spectral data.

5. Modeling the data

For more than two decades spot models have successfully reproduced the periodic brightness variations of RS CVn, BY Dra, W UMa, Algol, and even T Tau stars (Eaton 1991). However the modeling of the light curves suffers from non-uniqueness (Strassmeier 1990). The spectral lines contain more information about the surface inhomogeneity of the stars but it is more difficult to extract it. Different approaches were developed for surface mapping on the basis of the spectral lines: Doppler imaging (Vogt & Penrod 1983), bisector analysis (Toner & Gray 1988) and correlative analysis (Dempsey et al. 1992). Although the potential of these methods is good, they have not been widely applied because of the strong requirements for the quality of the spectral data.

The spectra of the most active stars do not satisfy the foregoing requirements. That is why light curve modeling remains the only method for their surface mapping. There are different packages for light curve synthesis but their algorithm is nearly the same.

We used the standard package of Bradstreet (1993) for a light curve modeling of our data fixing, a priori, two parameters:

(a) On the base of both the mass function $f(m)$=0.082 $M_{\odot}$ and the spectral type G3V of the primary it may be concluded that its mass is around $1M_{\odot}$. The deep eclipse minima of XY UMa are possible for a high orbital inclination $i > 80°$. Then the mass of the secondary should be 0.58-0.62 $M_{\odot}$. This value corresponds to its K5V classification. So, we assumed a mass ratio of q=0.6.

(b) The temperature of the primary T_1=5780 K is determined from its spectral type.

The rest parameters of XY UMa configuration, determined by fitting its light curves by different authors, range in quite wide intervals: inclination $77 - 88^{\circ}.2$; relative primary radius 0.325-0.41; relative secondary radius 0.164-0.24; temperature of the secondary 4000-4600 K. That is why we could not fix in advance the values of the foregoing parameters and had to vary them. The aim of this first step of the modeling procedure was to get a fit of the synthetic clean (without spots) curve with those features of the observational light curve that are most independent of the presence of spots. We assume that these are the inclination of the steeper branches of the two minima, the light level of the primary minimum and the level of maximum brightness at phase 0.7.

We obtained a satisfactory result with parameters almost equal to those of Hilditch & Bell (1994): the relative radii of the two stars $r_1(back) = 0.363$ and $r_2(back) = 0.211$; temperature of the secondary 4100 K; inclination $80°$. These values mean that the relative luminosities of the primary and secondary star are 0.947 and 0.053 respectively that is in good agreement with the estimation of Budding & Zeilik (1987).

In order to take into account the contribution of the spots and to get a fit to the observational light curve during the whole orbital cycle we built the distortion curve as a difference between the observational data and the synthetic clean (without spots) curve. The corresponding three curves in I colour are shown in Fig. 8.

We interpreted the distortion curve in the following way: (a) One spot on the primary (if the spots were on the secondary weak star then their effect should be negligible) could fit the first minimum of the distortion curve at phase range 0.8-1.2. It is covered at least partially at the primary eclipse by the secondary star (see phase range 0.98-1.03 of the distortion curve), i.e. it is situated at low latitude and is best visible at phase 0.05; (b) Second spot is necessary to fit the second minimum of the distortion curve at phase range 0.25-0.7. The phase of its best visibility is around 0.45.

The different contributions of the two spots on the distortion curve imply different sizes and/or latitudes and/or temperatures. In order to fit the distortion curve and the whole light curve respectively we varied these parameters in the following way. Usually the temperature difference between the star and spots of the RS CVn systems is around 500-1500 K and we varied this parameter in these limits. The spot sizes α were varied from $10°$ to $30°$ and the latitudes of the spot centers in an arbitrary way. Appropriate coefficients of the proximity effects (reflection, gravity darkening) and limb-darkening effect both for each star and each colour were used.

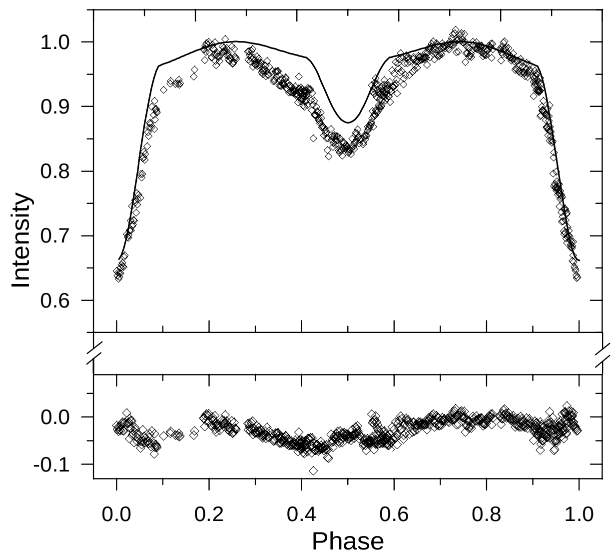

Fig. 8. Observational and synthetic clean (without spots) I light curve (top) and corresponding distortion curve (down). The observational data are converted from magnitudes to intensities and phase shifted by 0.037 in respect to the ephemeris (1).

Many solutions were obtained for each colour separately. But the main difficulty was to find a fit for all the colours with the same spot parameters. It should be noted that all previous analyses for this star are made mostly for one-colour curve (Budding & Zeilik 1987; Zeilik et al. 1988; Hilditch & Bell 1994; Erdem & Gudur 1998) or surprisingly the obtained parameters corresponding to the different colours have turned out quite different (for instance, Zeilik et al. 1990 obtain for simultaneous observations $\alpha(B) = 16°$ but $\alpha(V) = 9°$).

We obtained a good fit for all colours by two spots with parameters: spot sizes $20°$ and $10°$; spot latitudes $25°$ and $48°$; spot longitudes $15°$ and $165°$; spot temperatures 4630 K and 4330 K. It is shown in Fig. 9 as a blank line.

$Note$. A good fit was obtained also with one spot on the primary. The spot parameters were respectively: angular size $50°$, latitude $41°$, longitude $232°$ and temperature T^{sp}=5620 K. In order to get a fit in all colours we had to add a third light source. Because the huge spot size, the very small temperature difference between the spot and surrounding photosphere (only 180 K) and the artificial third light source we consider that this one-spot solution is not physically reasonable.

The results of the light curve modeling raise the question about the connection of the two cool photospheric spots and the orbital behaviour of the $H\alpha$ profile. It is known that the chromospheres of the RS CVn stars are nonhomogeneous and the regions above the photospheric cool spot are sources of $H\alpha$ and CaII H and K emission. Then we may attribute the variability of the $H\alpha$ profile to the contribution of the emission of the chromospheric regions above the spots. They could be sources of an emission feature that fills in the photospheric absorption line and moves across it as the primary star rotates. Some facts support this assumption: (a) The contribution of the spots should

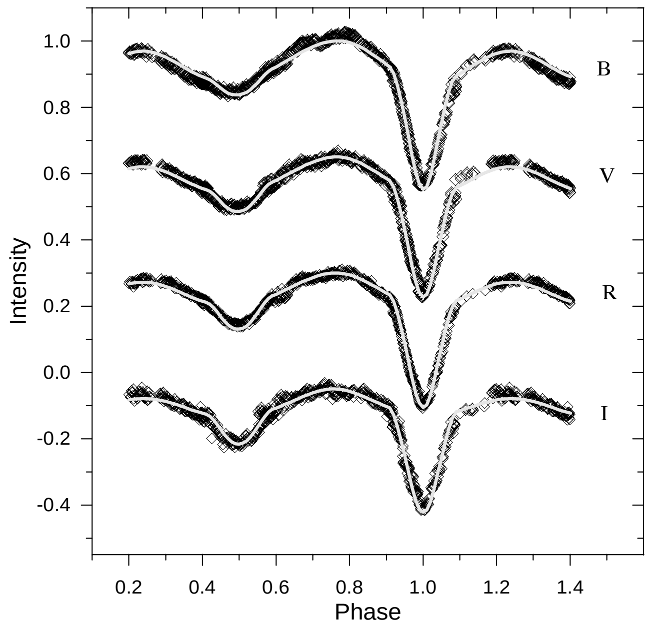

Fig. 9. The synthetic light curves (solid blank lines) and observational light curves (blank diamonds). The observational data are converted from magnitudes to intensities and phase shifted by 0.037 in respect to the ephemeris (1).

be minimal at the phases 0.23 and 0.68 when the profiles do are undistorted (i.e. symmetric); (b) The central bump of the profile at the phase of the maximum visibility of the larger spot (0.05) could be explained as a result of the emission of the chromospheric region above it.

6. Conclusions

We found the following signs of activity of XY UMa:

(1) The light curve of the star is asymmetric. This is the photometric manifestation of the photospheric activity of its primary star. Two cool spots with sizes 20° and 10°; temperatures 4630 and 4330K reproduced well the light curves in all colours. The total spotted area is around 3% of the whole primary surface.

(2) The observed $H\alpha$-profile is quite wide and shows variable asymmetry during the orbital cycle. The corresponding radial velocity curve is sinusoidal with semiamplitude $K_1 = 120.7\pm2.9$ km/s. The phase behaviour of the $H\alpha$-profile implies contribution of emission of the chromospheric regions above the photospheric spots.

The high level of activity of XY UMa is probably due to its rapid rotation, duplicity and relative strong magnetic field.

Acknowledgements. The authors are grateful to Prof. St. Zola for the help in the modeling and useful discussion. This work was partially supported by grants of joint CEEPUS project BG-2 and project $\Phi-634$ of Bulgarian Science Foundation. The stay of the first two authors in Poland was supported by Krakow Pedagogical University.

References

Antov A., Konstantinova-Antova R., 1995, In: Bode M.F. (ed.) Robotic Observatories-Workshop on Robotic Telescopes. Ireland, Pergamon Press, p. 69
Arevalo M., Lazaro C., 1990, AJ 99, 983
Borkowski J., 1988, Internal report of Torun (Poland)
Bradstreet D., 1993, In: Milone E. (ed.) Light Curve Modeling of Eclipsing Binary Stars. Springer-Verlag, New York, p. 151
Budding E., Zeilik M., 1987, ApJ 319, 827
Dempsey R., Bopp B., Strassmeier K., et al., 1992, ApJ 392, 187
Drake S.A., Simon T., Linsky J.L., 1986, AJ 91, 1229
Eaton J., 1991, In: Byrne P., Mullan D. (eds.) Surface Inhomogeneities on Late-type Stars. Springer, Berlin
Erdem A., Gudur N., 1998, A&AS 127, 257
Geyer E., 1976, In: Eggleton P., Mitton S., Whelan J. (eds.) Structure and Evolution of Close Binary Systems. p. 313
Geyer E., 1977, Ap&SS 48, 137
Geyer E., 1980, In: Plavec M., Popper D., Ulrich R. (eds.) Close Binary Stars: Observations and Interpretation. p. 423
Geyer E., Hoffman M., 1981, Mitt. Astr. Ges. Humb. 52, 70
Geyer E., Metz K., 1977, Ap&SS 52, 351
Geyer E., Kippenhahn R., Strohmeier W., 1955, Kleine Veröffentl. Remeis Sternwarte Bamberg No.9
Gray D., 1992, In: The observation and analysis of stellar photospheres. Cambridge Astrophysics Series 20, p. 248
Hall D., 1976, In: Fitch W. (ed.) IAU Colloquium 29, Multiple Periodic Variable Stars. Reidel, Dordrecht, p. 287
Hall D., Kreiner J., 1980, Acta Astron. 30, 387
Hilditch R., Bell S., 1994, MNRAS 267, 1081
Hilditch R., Collier Cameron A., 1995, MNRAS 277, 747
Jeffries R.D., Collins C., Elliot K.H., Pittard J.M., Taylor S.B., 1995, IBVS No. 4277
Kreiner J., Krzesinski J., Pokrzywka B., et al., 1993, In: Elliot I., Butler C. (eds.) IAU Coll No 136, Poster Papers on Stellar Photometry. Institute for Advanced Studies, Dublin, p. 80
Krzesinski J., Wojcik K., 1993, A&A 280, 338
Li Q.S., Zhang X.Y., Zhang R.X., 1989, IBVS No. 3374
Pojmanski G., Geyer E., 1990, Acta Astron. 40, 245
Rahunen T., Vilhu O., 1982, In: Kopal Z., Rahe J. (eds.) IAU Colloquium 69, Binary and Multiple stars as Tracers of Stellar Evolution. Reidel, Dordrecht, p. 289
Rainger P., Hilditch R., Edwin R., 1991, MNRAS 248, 168
Singh K., Drake S., White N., 1996, AJ 111, 2415
Smirnov O., Piskunov N.E., Afanasyev V.P., Morozov A.I., 1992, In: Worrall D.M. Biemesderfer C., Barnes J. (eds.), ASP Conf. Ser. Vol. 26, Astronomical Data Analysis Software and Systems I, p. 344
Southwell K., Still M., Connon Smith R., Martin J., 1995, A&A 302, 90
Strassmeier K., 1990, ApJ 348, 682
Szymanski M., Udalski A., 1989, Acta Astron. 39, 1
Toner C., Gray D., 1988, ApJ 334, 1008
Vogt S., Penrod D., 1983, PASP 95, 565
Zeilik M., Batuski D., Elston R., et al., 1982, IBVS No. 2169
Zeilik M., Elston R., Henson G., 1983, AJ 88, 532
Zeilik M., Cox D., De Blasi C., et al., 1988, IBVS No. 3200
Zeilik M., De Blasi C., Cordon S., Ledlow M., 1990, IBVS No. 3535